Sensorless FCS-MPC-Based Speed Control of a Permanent Magnet Synchronous Motor Fed by 3-Level NPC

Sajad Saberi, Behrooz Rezaie*

Department of Computer and Electrical Enginnering, Babol Noshirvani Univercity of Technology, P. O. Box: 47148-71168, Babol, Mazandaran, Iran.

A B S T R A C T

This paper presents a sensorless speed control algorithm based on Finite Control Set Model Predictive Control (FCS-MPC) for Permanent Magnet Synchronous Motor (PMSM) fed by a 3-level Neutral-Point Clamped (NPC) converter. The proposed scheme uses an anti-windup Proportional-Integral (PI) controller concept to generate the reference electromagnetic torque using the error of speed. Then, FCS-MPC uses this torque reference and other parameters such as a current limitation, neutral point voltage unbalance, and switching frequency to control the converter gate signals. Also, an Adaptive Nonsingular Fast Terminal Sliding Mode Observer (ANFTSMO) was employed to estimate rotor position precisely in positive (clockwise) and negative (counterclockwise) speed to eliminate the encoder. The proposed algorithm has fast dynamics and low steady-state error. Moreover, torque fluctuation and current distortion reduced compared with Space Vector Pulse Width Modulation (SVPWM) based speed control and Direct Predictive Speed Control (DPSC). Simulation results using MATLAB/SIMULINK® demonstrate the performance of the proposed scheme.

1. INTRODUCTION

Wind energy is the fastest growing among all renewable energy systems and it has become possible due to the rapid advances in the size of wind generators as well as the developments in power electronics [1]. Variable-speed Wind Energy Conversion Systems (WECS) can be controlled over a wide range of wind speeds to facilitate their operability at maximum power coefficients, thus allowing them to obtain larger energy capture from the wind [2, 3]; therefore, speed control is the vital factor of Maximum Power Point Tracking (MPPT) of this type of WECSs [4, 5].

The most promising topology for variable WECSs is the direct-driven, multi-pole Permanent Magnet Synchronous Machine (PMSM) [5] which is characterized by more advantages than fixed-speed ones such as higher power density, fast dynamic response, improved efficiency, and reduced mechanical stress [5-7].

Field-Oriented Control (FOC) and Direct Torque Control (DTC) are the most common strategies to control PMSMs [8, 9]. Windup problem and bandwidth limitation (due to existence of modulator) make FOC a non-ideal controller choice [10]. DTC uses switching table to control motor torque directly. Given that output voltage vectors are not always optimal, this method suffers from high torque and stator flux ripples [11, 12].

While the complexity of converters increases, the necessity of applying advanced control strategies that are capable of

considering multivariable systems and handling additional control objectives is undeniable [13]. Multivariable structure, excellent performance in the presence of nonlinearities, and constraints consideration make MPC one of the best choices for drive systems [14, 15]. Finite Control Set Model Predictive Control (FCS-MPC) is one of the MPC methods that takes advantage of the fact that the number of possible switching states is limited; therefore, it is possible to predict the effect of each Voltage Space Vector (VSV) to determine the best VSV for the next sampling time [16].

FCS-MPC has been used to control the current in several converter topologies [16-19]. Because of the inherent sluggish behavior of the mechanical system, the ordinary Proportional Integral (PI) controller does not provide a fast response to reference speed change [19]. To overcome this problem, Direct Predictive Speed Control (DPSC) without cascade structure has been introduced [20-22].

A DPSC strategy directly controls the speed of the motor and achieves high-speed control dynamics [13]. Compared to current dynamic, mechanical dynamic is very slow and this significant difference between time constants leads to torque fluctuation and current distortion. Therefore, the designer needs to consider a longer prediction horizon for DPSC [23]. Longer prediction horizon means more different switching states that increase the computation time so drastically that real-time implementation is not feasible in general [24]. In [13], a DPSC method with a shorter prediction horizon was used to control the speed of a PMSM fed by 3-level NPC inverter. Results in [13] were acceptable, but two-step prediction horizon means $27^2 = 729$ different switching

*Corresponding Author's Email: brezaie@nit.ac.ir (B. Rezaie)
URL: http://www.jree.ir/article_122410.html

states, which is far from 27 switching states for one-step prediction horizon; therefore, this paper proposes a one-step prediction horizon method.

One of the key factors of all speed control schemes of the PMSM is the precise sensing of speed and position using a dedicated external sensor or the exact estimation using a fast and accurate observer. Eliminating encoder used to measure the speed and position of the shaft increases the reliability and applicability of PMSM and leads to schemes with more compact constructions and lower costs [25].

The most common method for the position and speed estimation of PMSM is the back electromotive force (back-EMF) method [26, 27]. Despite the simplicity of this method, it yet shows excellent results in high-speed applications [28, 29]. However, one of the well-known problems of this method is the dependency of back-EMF on the speed of the rotor. When motor works in the low-speed range, since back-EMF is small, accurate estimation of position becomes a challenging task [27-29]. In [23], a startup strategy was designed to provide a better estimation at low speeds. In [31], an active flux estimator was used to ensure a better estimation at lower speeds. However, this method is not able to estimate position in the reverse mode.

In this paper, a full range position and speed estimator using an Adaptive Nonsingular Fast Terminal Sliding Mode Observer (ANFTSMO) [25] was employed to estimate the PMSM rotor angle and speed without an encoder. ANFTSMO can not only solve the chattering problem in the low-speed region, but also track the rotor angle at reverse speeds quickly, accurately, and without chattering [25].

To control the speed of PMSM in the presence of current/torque limitation, in the proposed method, first, we design a reference torque to use in FCS-MPC; then, a cost function using current references, torque reference, torque constraint, and switching constraint is designed. By replacing the speed error term with the electromagnetic term in the cost function, the necessity of using multiple horizons is obviated and the proposed method becomes almost as fast as a predictive speed control scheme with lower torque oscillation, current distortion, and steady-state error.

The main contribution of the paper is as follows:

- Rotor position estimation using ANFTSMO
- Designing a discrete electromagnetic torque reference signal for FCS-MPC
- Proposing a new objective function for FCS-MPC-based speed controller.

It is worth mentioning that the novelty of the paper is in utilizing the designed torque reference as a part of the cost function to minimize the oscillation of speed and torque.

The organization of the paper is as follows. Section 2 gives a description of model including PMSM and inverter and their equations. Section 3 introduces the FCS-MPC algorithm and the proposed method. Section 4 explains cost function terms and considerations. Section 5 introduces and discusses simulation results. Section 6 concludes the paper.

2. SYSTEM DESCRIPTION

Fig. 1 shows a topology including PMSM fed by 3-level NPC. The PMSM and inverter models are described in the following subsections.
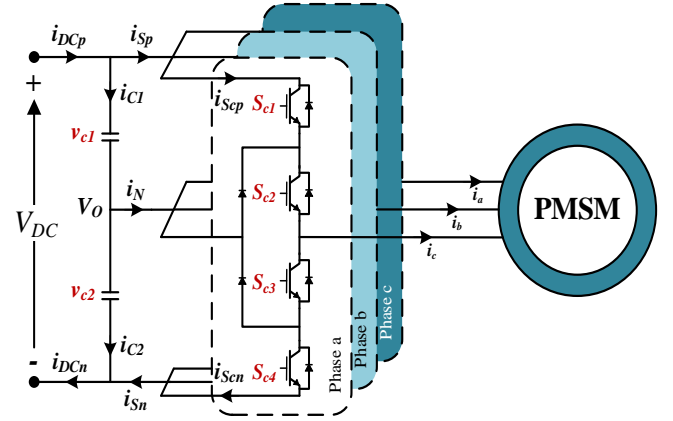

Figure 1. PMSM fed by 3-level NPC topology

2.1. PMSM model

By assuming a Surface-Mounted PMSM (SPMSM) with the same inductance for d and q axes, the dynamic model for the SPMSM in the d-q reference frame can be described as follows [16]:

$$\frac{di_d}{dt} = \frac{1}{L_s}\left(v_d - R_s i_d + \omega_e L_s i_q\right)$$
$$\frac{di_q}{dt} = \frac{1}{L_s}\left(v_q - R_s i_q - \omega_e L_s i_d - \omega_e \psi_{mg}\right)$$
$$T_e = \frac{3}{2} Z_p \psi_{mg} i_q \tag{1}$$
$$\frac{d\omega_e}{dt} = \left(\frac{Z_p}{J_m}\left(T_e - T_L\right) - \frac{B_v}{J_m}\omega_e\right)$$

A discrete model of PMSM is needed to predict the future values of current and torque for FCS-MPC. To decrease the calculation burden, the model can be rewritten in discrete time using a simple discretization method like the Euler method [32].

$$i_d[k+1] = \left(1 - \frac{T_s R_s}{L_s}\right) i_d[k]\ldots$$
$$+ \frac{T_s}{L_s} v_d[k] + T_s \omega_e[k] i_q[k]$$
$$i_q[k+1] = \left(1 - \frac{T_s R_s}{L_s}\right) i_q[k] + \frac{T_s}{L_s} v_q[k]\ldots \tag{2}$$
$$+ T_s \omega_e[k] i_q[k] - \frac{T_s \psi_{mg}}{L_s}\omega_e[k]$$
$$T_e[k+1] = \frac{3}{2} Z_p \psi_{mg} i_q[k+1]$$

2.2. Inverter mode

The power circuit of NPC inverter for one phase is shown in Figure 1. S_{xq} represents the switching state of phase x and switch q with x={a, b, c} and q={1, 2, 3, 4}. Table 1 shows the values of S_{xq} and its equivalent voltages. For three phases of this inverter, 27 switching states are generated [33]. It is worth mentioning that to prevent short circuit, $S_{x3} = 1-S_{x1}$ and $S_{x4} = 1-S_{x2}$.

Table 1. Switching table of one phase of NPC inverter

S_x	S_{x1}	S_{x2}	S_{x3}	S_{x4}	U_x
P = 1	1	1	0	0	$V_{dc}/2$
0	0	1	1	0	0
N = −1	0	0	1	1	$-V_{dc}/2$

To use in (1), one needs to convert it to and using Park and Clarke transformation as follows:

$$v_{dq} = \begin{bmatrix} v_d & v_q \end{bmatrix}^T = MDU_x$$

$$M = \begin{bmatrix} \cos\theta & -\sin\theta \\ \sin\theta & \cos\theta \end{bmatrix}$$

$$D = \frac{2}{3}\begin{bmatrix} 1 & -1/2 & -1/2 \\ 0 & \sqrt{3}/2 & -\sqrt{3}/2 \end{bmatrix}$$

(3)

where D is Clarke transformation, M is the Park transformation matrix and θ is the electrical angle of the rotor [8].

Unbalanced neutral point voltage V_o has negative impact on the output voltage and semiconductor switch stress [34]. FCS-MPC has the ability to control V_o by predicting the voltage of the neutral point using 3-phase currents and switching states as follows [34]:

$$\frac{dV_O}{dt} = \frac{dV_{c1}}{dt} - \frac{dV_{c2}}{dt} = \frac{1}{C}\left\{\left(I_{Sp} - I_{Sn}\right)\right\}$$

$$V_O[k+1] = V_O[k] + \frac{T_s}{C}\left(I_{Sp}[k] - I_{Sn}[k]\right)$$

(4)

3. FCS-MPC DESCRIPTION

Figure 2 illustrates the operating principle of FCS-MPC [35]. Due to the finite number of switching states S_i, FCS-MPC can predict all possible system states x^p over a sampling period T_s based on system model and measured values. Then, depending on the objectives, a cost function C can be defined to discover the best possible switching.

As an example, considering Figure 2 in the first step, $x_2^p[k+1]$ is closest to the reference x^{ref}; thus, S_2 is selected and applied at t = k. Following the same procedure, S_3 will be selected for the second step and used at t = k + 1.
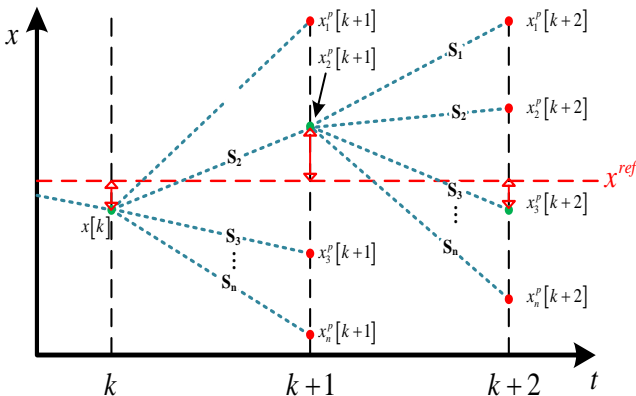
Figure 2. Operating principle of FCS-MPC

4. COST FUNCTION DESIGN

According to the FCS-MPC scheme, cost function has a significant effect on system performance [16]. By properly selecting the cost function, FCS-MPC can control multiple objectives at the same time. However, proper selection of the items and weightings is a challenging task. In this section, items of the cost function are discussed.

4.1. Tracking term

The main objective of the controller is to control the speed of PMSM. First, a reference is designed for electromagnetic torque. The design procedure is based on an anti-windup PI controller concept [36].

$$T_e^{ref}[k+1] = T_e^{ref}[k] + k_1\left(e_\omega[k] - e_\omega[k-1]\right)...$$
$$+ k_2 T_s\left(e_w[k] + \overline{e}[k]\right)$$

(5)

where T_e^{ref} is the electromagnetic torque reference to use in FCS-MPC, k_1 and k_2 are coefficients, and e_ω and $\overline{e}$ are as follows:

$$e_\omega[k] = \omega^{ref}[k] - \omega[k]$$

$$\overline{e}[k] = \begin{cases} T_e^{max} - T_e^{ref}[k] & T_e^{ref}[k] > T_e^{max} \\ -T_e^{max} - T_e^{ref}[k] & T_e^{ref}[k] < -T_e^{max} \\ 0 & \text{o.w} \end{cases}$$

(6)

After reference generation for T_e, its error can be used in the cost function.

$$e_{T_e} = T_e^{ref}[k+1] - T_e[k+1]$$

(7)

In surface-mounted PMSM with $L_d = L_q$ [6], the d-axis current does not affect electromagnetic torque and can be controlled independently. Thus, we can consider an error for d-axis current control.

$$e_{i_d} = i_d^{ref}[k+1] - i_d[k+1]$$

(8)

It is worth mentioning that $i_d^{ref}[k+1]$ is not accessible and if we use $i_d^{ref}[k]$ instead, it may lead to a delay in the system. Here, extrapolation method is used to build $i_d^{ref}[k+1]$ from current and past values of i_d^{ref} as follows [37]:

$$i_d^{ref}[k+1] = 3i_d^{ref}[k] - 3i_d^{ref}[k-1] + i_d^{ref}[k-2]$$

(9)

By combining e_{T_e} and e_{i_d} into one function, tracking term of the cost function will be as (10):

$$C_T = \begin{bmatrix} e_{i_d} & e_{T_e} & e_\omega \end{bmatrix} \begin{bmatrix} \lambda_{i_d} & 0 & 0 \\ 0 & \lambda_{T_e} & 0 \\ 0 & 0 & \lambda_\omega \end{bmatrix} \begin{bmatrix} e_{i_d} \\ e_{T_e} \\ e_\omega \end{bmatrix}$$

(10)

where λ_{i_d}, λ_{T_e}, and λ_ω are the weighting factors.

4.2. Zero term

Zero term is a part of the cost function that should be kept at zero. Here, only the neutral point voltage is considered for this term.

$$C_Z = \lambda_{V_o} \left(V_o \right)^2 \tag{11}$$

4.3. Constraint term

The constraint term may consist of multiple parts such as current limitation, torque limitation, and switching limitation. We considered the current limitation and switching limitation using (12) and (13).

$$C_{CI} = \begin{cases} \lambda_{I_m} \left(\sqrt{i_d^2 + i_q^2} - I_m \right) & \sqrt{i_d^2 + i_q^2} > I_m \\ 0 & o.w \end{cases} \tag{12}$$

$$C_{CS} = \lambda_S \left(\sum_{x=a,b,c} \left| S_x[k+1] - S_x[k] \right| \right) \tag{13}$$

where λ_{I_m} and λ_S are the weighting factors.

Using C_{CI}, we limit the current to the maximum allowed value and C_{CS} helps have a lower switching frequency by considering switch state as a variable. Thus, if we have two different switching with the same cost, the one with a lower switching change will be chosen.

As an example, if the last switching is S = [1 0 -1] and in next sampling, S_n = [0 0 -1] and S_m = [1 1 -1] have the same cost, the former one will be chosen, because it has just one switching in phase a and switching states in phase b and c will remain unchanged.

By incorporating C_{CI} and C_{CS} into one term, the constraint term is written as follows:

$$C_C = C_{CI} + C_{CS} \tag{14}$$

Finally, by considering the tracking term, the zero term, and the constraint term in one equation, the cost function to be minimized using FCS-MPC becomes

$$C = C_T + C_Z + C_C \tag{15}$$

Remark: A combination of multiple variables in a single cost function is not a straightforward task when they have different natures (in units or values). Finding optimal weighting factors is still an open problem, but there are some methods to find these factors correctly [38, 39]. Designing weighting factors is not in the scope of this paper and in this work, factors are designed using normalization and multiple simulations.

5. SIMULATION AND RESULTS

To demonstrate the performance of the proposed method in this section, the method is compared with two other methods, i.e., a DSPC using FCS-MPC introduced in [20] and an FOC method with a cascade structure using anti-windup PI as speed controller and SVPWM modulator [40]. Moreover, for the latter one, a system without a modulator is considered to

check the ideal case without switching. In these references, similar to our study, one-step prediction horizon has been used to decrease the oscillation.

Figure 3 illustrates the block diagram of the proposed method, and Figure 4 shows the flowchart for more details. Also, the parameters of the PMSM, inverter, and controller are presented in Table 2. Furthermore, the angle of the rotor is estimated using the method in [24] for all three controller schemes.
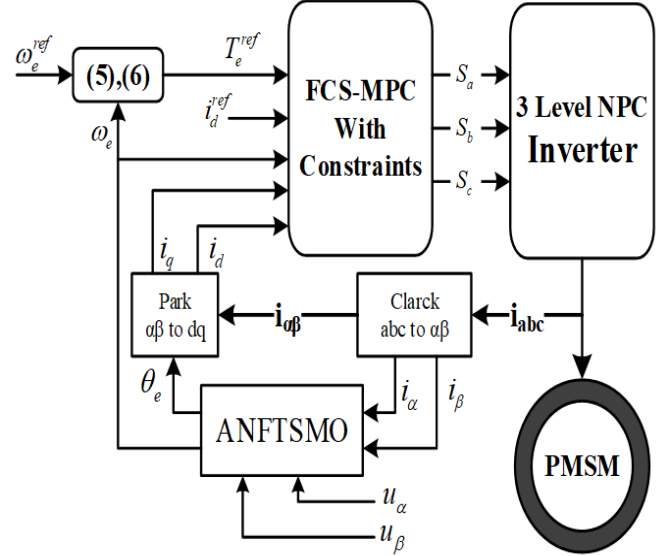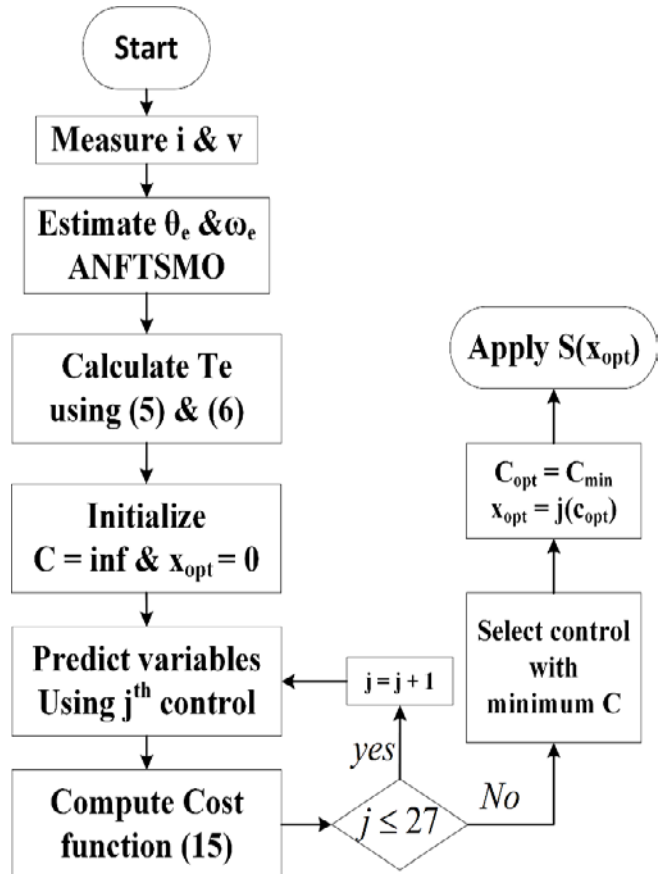

Figure 3. Block diagram of the proposed method

Figure 4. Proposed method flowchart

Table 2. System and controller parameters

Variable	Parameter	Value	Symbol
Sampling time	T_s	10	μs
Stator resistance	R_s	6.8	Ω
Stator inductance	L_s	8	mH
Flux linkage	ψ_{mg}	0.41	web
Pair poles	Z_P	3	
Moment of inertia	J_m	0.0212	kg/m²
Viscose damping	B_v	0.31	Ns/m
DC voltage	V_{DC}	120	V
Current limitation	I_{max}	6.5	A
Torque limitation	T_{em}	12	Nm
Proportional factor	k_1	30	
Integral factor	k_2	10000	

Figure 5 shows the reference value of speed, reference value of T_e along with actual and estimated values of motor shaft position during simulation. It is clear that the ANFTSMO estimated rotor position accurately not only at low and high speeds but also during speed direction change.
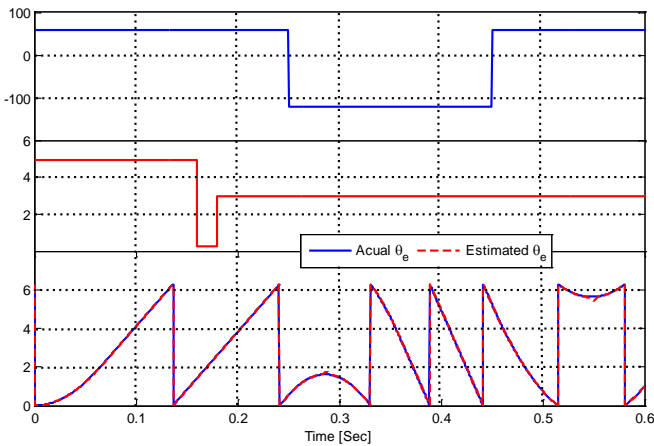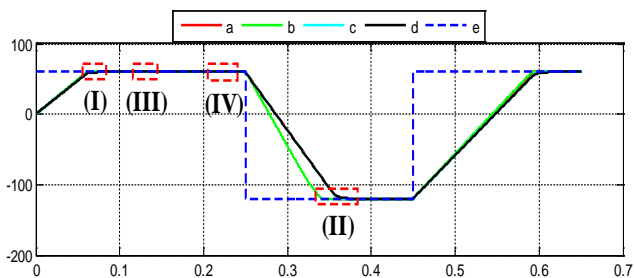

Figure 5. Reference for speed and mechanical torque and the rotor angle

Figure 6 shows speed change during the simulation for four methods as mentioned above and for more details, Figure 7 illustrates zoomed areas of Figure 6 defined with red dotted rectangles.

Figure 6. Speed change during simulation, a) Proposed method, b) DSPC, c) Ideal FOC, d) SVPWM FOC, and e) Reference speed

Section (I) of Figure 7 shows the step change of the reference speed. As can be seen, due to the slow dynamic of speed, compared to current dynamic, the DPSC method has oscillatory behavior with the one-step horizon. Moreover, the FOC method has a lower speed even by considering the ideal case, without switching and modulator. The main reason behind this lower speed dynamic is the cascade scheme, which forces the designer to have a lower bandwidth in outer loop. Also, by adding the modulator and switching, the FOC has a lower speed than the ideal case. However, the proposed method has a faster dynamic than the FOC method and smaller overshoot and lower oscillation than original DPSC. When the speed error term e_ω reaches near zero, the torque component added to the cost function, with a faster dynamic, will have greater impact on the optimal value for switching selection; thus, the sluggish nature of the cost function is almost obviated and motor speed has very lower oscillation than DPSC.

Section (II) of Figure 1 shows step down of speed and has almost the same behavior as step up change. Section (III) shows speed change during mechanical torque variation, it can be seen that FOC and the proposed method have the same behavior. Finally, Section (IV) shows the steady-state response of the system for the proposed method and FOC. Because of the optimal selection of voltage vectors, the proposed method has very lower steady-state error; however, in return, it suffers from variable switching frequency unlike FOC. To have a quantitative criterion for speed and torque distortion, using the Mean Square Error (MSE) for the speed and torque variables, as described in (16), the results can be shown in Table 3. It can be observed that the proposed method has a lower speed and torque distortion than SVPWM. This advantage is because the designed torque reference is considered as part of the cost function to minimize the oscillation of speed and torque.

$$\text{Speed MSE} = \sum_{j=1}^{N}\left(\omega_e(j) - \omega_e^{ref}\right)^2$$

$$\text{Torque MSE} = \sum_{j=1}^{N}\left(T_e(j) - T_e^{ref}\right)^2 \tag{16}$$
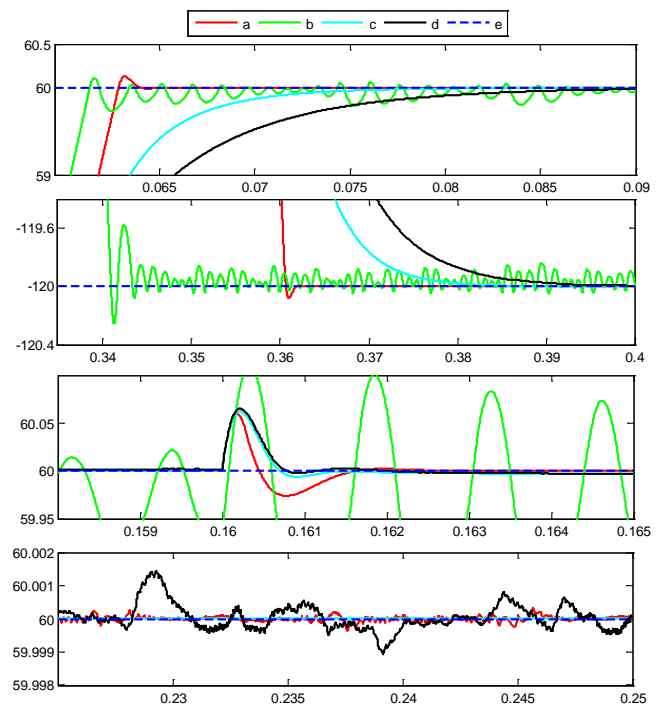

Figure 7. Zoomed area of Figure 3, (I): Motor speed during reference speed step-up variation, (II): Motor speed during reference speed step-down variation. (III): Motor speed during load torque variation, and (IV): Motor speed in a steady state, a) Proposed method, b) DPSC, c) Ideal FOC, d) SVPWM FOC, and e) Reference speed

Table 3. Speed and torque MSE for the proposed method and SVPWM method

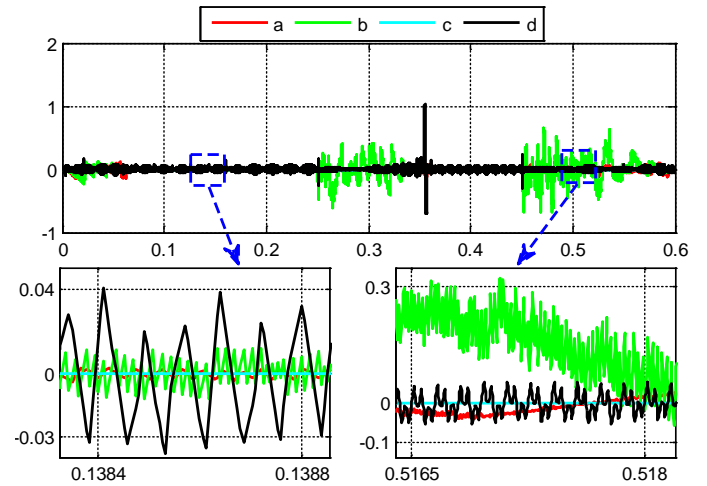|	Proposed method	SVPWM
Speed MSE	$6.85e^{-5}$	$160e^{-5}$
Torque MSE	0.0348	0.176

Figure 8 illustrates variations of electromagnetic torque T_e during simulation and for more details, Figure 9 shows the zoomed area of red rectangles in Figure 8.

From Figure 9, Sections (I) and (II), it can be seen that in step-up and step-down speed changes, because of the nature of the predictive control, the proposed method has no overshoot or under-shoot. Also, in the DPSC, there is a high gain fluctuation in T_e, which can reduce the life expectancy of motor shaft.

Section (III) of Figure 9 illustrates the steady-state performance of T_e for all the methods mentioned above. Despite the DPSC which has high oscillation because of the difference between mechanical and electrical time constants as well as the ideal FOC which experiences no oscillation, the proposed method is subject to much less oscillation than SVPWM FOC.
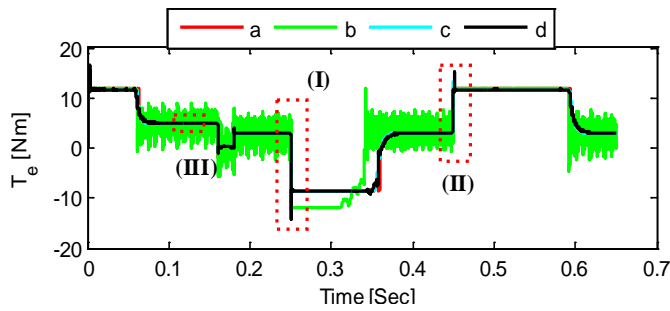
Figure 8. Electromagnetic torque variation during the simulation, a) proposed method, b) DPSC, c) Ideal FOC, and d) SVPWM FOC
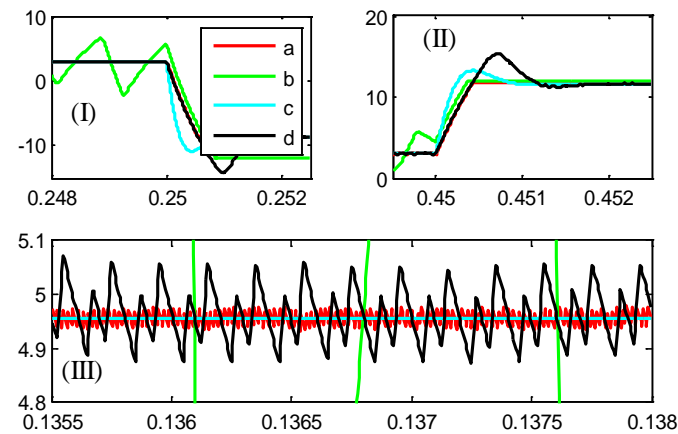
Figure 9. Zoomed area of Figure 5, (I): during step-down reference speed, (II): during step-up reference speed, (III): in steady-state, a) proposed method, b) DPSC, c) Ideal FOC, d) SVPWM FOC

For surface-mounted PMSMs, one of the controller's objectives is to keep d-axis current at zero to satisfy the MTPA criteria [41]. Figure 10 shows i_d during simulation, showing that in the steady-state and transient phases, the proposed method has a better performance than other methods, except ideal FOC without switching components.

Figure 10. d-axis current variation during simulation time and zoomed areas, a) proposed method, b) DPSC, c) Ideal FOC, and d) SVPWM FOC

6. CONCLUSIONS

In this work, an encoder-less FCS-MPC-based speed control algorithm was proposed for a PMSM fed by a 3-level NPC converter. The controller used an anti-windup PI controller concept to generate reference torque using the error of speed; then, FCS-MPC used this torque and other parameters to control converter gates.

Simulation results demonstrated the effectiveness of the method in the transient and steady state phases. The method has not only a fast response during reference variation but also much lower overshoot or undershoot than FOC method. Moreover, compared with the recent methods like DPSC, the proposed method has much less oscillation in a steady state in both speed and torque characteristics. Future research could continue to explore experimental results and compare the results with methods that used multiple prediction horizon.

7. ACKNOWLEDGEMENT

NOMENCLATURE

i_d, i_q	Stator current in dq Ref. frame
v_d, v_q	Stator voltage in dq Ref. frame
R_s	Stator resistance
L_s	Stator inductance
ω_e	Electrical rotor speed
θ	Electrical angle of the rotor
T_e	Electromagnetic torque
T_L	Load torque
Z_P	Number of pole pairs
J_m	Inertia coefficient
B_v	Friction coefficient
ψ_{mg}	Flux linkage
T_s	Sampling time
V_{DC}	DC voltage
I_{max}	Current limitation
T_{em}	Torque limitation
Greek letters	
λ_x	Weighting factors and x = {i_d, i_q, T_e, V_o, I_m}
Subscripts	
$.^{ref}$	Reference value
Abbreviation	

WECS	Wind Energy Conversion System
MPPT	Maximum Power Point Tracking
PMSM	Permanent Magnet Synchronous Machine
FOC	Field-Oriented Control
DTC	Direct Torque Control
ANFTSMO	Adaptive Nonsingular Fast Terminal Sliding Mode Observer
MTPA	Maximum Torque Per Ampere
PI	Proportional Integral
MPC	Model Predictive Control
FCS-MPC	Finite Control Set - MPC
DPSC	Direct Predictive Speed Control
SPMSM	Surface-mounted PMSM

REFERENCES

1. Shi, S. and Lo, K.L., "An overview of wind energy development and associated power system reliability evaluation methods", *Proceedings of 48th International Universities' Power Engineering Conference (UPEC)*, Dublin, (2013), 1-6. (https://doi.org/10.1109/UPEC.2013.6714894).

2. Ackennan, T. and Soder, L., "An overview of wind energy status 2002", *Renewable and Sustainable Energy Reviews*, Vol. 6, No. 1-2, (2002), 67-128. (https://doi.org/10.1016/S1364-0321(02)00008-4).

3. Richardson, R.D. and McNerneyG, M., "Wind energy systems", *Proceedings of the IEEE*, Vol. 81, No. 3, (1993), 378-389. (https://doi.org/10.1109/5.241490).

4. Thongam, J.S., Tarbouchi, M., Beguenane, R., Okou, A.F., Merabet, A. and Bouchard, P., "An optimum speed MPPT controller for variable speed PMSG wind energy conversion systems", *Proceedings of IECON 2012-38th Annual Conference on IEEE Industrial Electronics Society*, Montreal, Quebec, (2012), 4293-4297. (https://doi.org/10.1109/IECON.2012.6389199).

5. Dastres, H., Mohammadi, A. and Rezaie, B., "Adaptive robust control design to maximize the harvested power in a wind turbine with input constraint", *Journal of Renewable Energy and Environment*, Vol. 8, No. 4, (2020), 30-43. (https://doi.org/10.30501/JREE.2020.224180.1093).

6. Barradi, Y., Zazi, K., Zazi, M. and Khali, N., "Control of PMSG based variable speed wind energy conversion system connected to the grid with PI and ADRC approach", *International Journal of Power Electronics and Drive Systems*, Vol. 11, No. 2, (2020), 953-968. (https://doi.org/10.11591/ijpeds.v11.i2.pp953-968).

7. Sain, C., Banerjee, A. and Biswas, P.K., "Modelling and comparative dynamic analysis due to demagnetization of a torque controlled permanent magnet synchronous motor drive for energy-efficient electric vehicle", *ISA Transactions*, Vol. 97, (2020), 384-400. (https://doi.org/10.1016/j.isatra.2019.08.008).

8. Holtz, J., "Advanced PWM and predictive control-An overview", *IEEE Transactions on Industrial Electronics*, Vol. 63, No. 6, (2016), 3837-3844. (https://doi.org/10.1109/tie.2015.2504347).

9. Li, Y., Qu, Y., Shi, H. and Meng, X., "An optimal switching table for PMSM DTC system using zero voltage vector", *Proceedings of 20th International Conference on Electrical Machines and Systems (ICEMS)*, Sydney, NSW, (2017), 1-5. (https://doi.org/10.1109/ICEMS.2017.8056409).

10. Linder, A. and Kennel, R., "Model predictive control for electrical drives", *Proceedings of IEEE 36th Power Electronics Specialists Conference*, Recife, (2005), 1793-1799. (https://doi.org/10.1109/PESC.2005.1581874).

11. Casdaei, D., Profumo, F. and Serra, G., "FOC and DTC: Two variable schemes for induction motors torque control", *IEEE Transactions on Power Electronics*, Vol. 17, No. 5, (2002), 779-788. (https://doi.org/10.1109/tpel.2002.802183).

12. Rahman, M.F., Haque, M.E. and Tang, L.X., "Problems associated with the direct torque control of an interior permanent-magnet synchronous motor drive and their remedies", *IEEE Transactions on Power Electronics*, Vol. 51, No. 4, (2004), 799-809. (https://doi.org/10.1109/tie.2004.831728).

13. Kakosimos, P. and Abu-Rub, H., "Predictive speed control with short prediction horizon for permanent magnet synchronous motor drives", *IEEE Transactions on Power Electronics*, Vol. 33, No. 3, (2018), 2740-2750. (https://doi.org/10.1109/TPEL.2017.2697971).

14. Sarailoo, M., Rezaie, B. and Rahmani, Z., "Fuzzy predictive control of three-tank system based on a novel modeling framework of hybrid systems", *Proceedings of the Institution of Mechanical Engineering, Part I: Journal of System and Control Engineering*, Vol. 228, No. 6, (2014), 369-384. (https://doi.org/10.1177/0959651814524948).

15. Jalili, S., Rezaie, B. and Rahmani, Z., "A novel hybrid model predictive control design with application to a quadrotor helicopter", *Optimal Control Applications and Methods*, Vol. 39, No. 4, (2018), 1301-1322. (https://doi.org/10.1002/oca.2411).

16. Rodriguez, J., Kazmierkowski, M.P., Espinoza, J.R., Zanchetta, P., Abu-Rub, H., Young, H.A. and Rojas, C.A., "State of the art of finite control set model predictive control in power electronics", *IEEE Transactions on Industrial Informatics*, Vol. 9, No. 2, (2013), 1003-1016. (https://doi.org/10.1109/TII.2012.2221469).

17. Wang, F., Mei, X., Rodriguez, J. and Kennel, R., "Model predictive control for electrical drive systems-an overview", *CES Transactions on Electrical Machines and Systems*, Vol. 1, No. 3, (2017), 219-230. (https://doi.org/10.23919/TEMS.2017.8086100).

18. Wang, L. and Gan, L., "Integral FCS predictive current control of induction motor drive", *IFAC Proceedings Volumes*, Vol. 47, No. 3, (2014), 11956-11961. (https://doi.org/10.3182/20140824-6-ZA-1003.00753).

19. Chai, S., Wang, L. andRogres, E., "A cascade MPC control structure for a PMSM with speed ripple minimization", *IEEE Transactions on Industrial Electronics*, Vol. 60, No. 8, (2013), 2978–2987. (https://doi.org/10.1109/TIE.2012.2201432).

20. Fuentes, E.J., Silva, C., Quevedo, D.E. and Silva, E.I., "Predictive speed control of a synchronous permanent magnet motor", *Proceedings of 2009 IEEE International Conference on Industrial Technology*, Gippsland, VIC, (2009), 1-6. (https://doi.org/10.1109/ICIT.2009.4939731).

21. Fuentes, E.J., Silva, C.A. and Yuz, J.I., "Predictive speed control of a two-mass system driven by a permanent magnet synchronous motor", *IEEE Transactions on Industrial Electronics*, Vol. 59, No. 7, (2012), 2840-2848. (https://doi.org/10.1109/TIE.2011.2158767).

22. Fuentes, E., Kalise, D., Rodriguez, J. and Kennel, R.M., "Cascade-free predictive speed control for electrical drives", *IEEE Transactions on Industrial Electronics*, Vol. 61, No. 5, (2014), 2176–2184. (https://doi.org/10.1109/TIE.2013.2272280).

23. Preindl, M. and Bolognani, S., "Model predictive direct speed control with finite control set of PMSM drive systems", *IEEE Transactions on Power Electronics*, Vol. 28, No. 2, (2013), 1007-1015. (https://doi.org/10.1109/TPEL.2012.2204277).

24. Bueno, E.J., Hernandez, A., Rodriguez, F.J., Giro, C., Mateos, R. and Cobreces, S., "A DSP- and FPGA-based industrial control with high-speed communication interfaces for grid converters applied to distributed power generation systems", *IEEE Transactions on Industrial Electronics*, Vol. 56, No. 3, (2009), 654-669. (https://doi.org/10.1109/TIE.2008.2007043).

25. Saberi, S. and Rezaie, B., "A full range permanent magnet synchronous motor position and speed estimation using adaptive non-singular fast terminal sliding mode observer", *Majlesi Journal of Energy Management*, Vol. 8, No. 4, (2019), 17-25. (http://journals.iaumajlesi.ac.ir/em/index/index.php/em/article/view/397).

26. Giri, F., AC electric motors control: advanced design techniques and applications, John Wiley and Sons, (2013), 59-76. (https://doi.org/10.1002/9781118574263).

27. Nahid-Mobarakeh, B., Meibody-Tabar, F. and Sargos, F.M., "Back EMF estimation based sensorless control of PMSM: Robustness with respect to measurement errors and inverter irregularities", *Proceedings of Industry Applications Conference, 39th IAS Annual Meeting. Conference Record of the 2004 IEEE*, Vol. 3, (2004), 1858-1865. (https://doi.org/10.1109/IAS.2004.1348723).

28. Hassan, M., Mahgoub, O. and Shafei, A.E., "ANFIS based MRAS speed estimator for sensorless control of PMSM", *Proceedings of 2013 Brazilian Power Electronics Conference, COBEP 2013*, (2013), 828-835. (https://doi.org/10.1109/COBEP.2013.6785211).

29. Xiao, D., Guan, D.Q., Rahman, M.F. and Fletcher, J., "Sliding mode observer combined with fundamental PWM excitation for sensorless control of IPMSM drive", *Proceedings of IECON 2014-40th Annual Conference of the IEEE Industrial Electronics Society, IEEE*, (2014), 895-901. (https://doi.org/10.1109/IECON.2014.7048607).

30. Nagarajan, V., Balaji, M. and Kamaraj, V., "Back-emf-based sensorless field-oriented control of PMSM using neural-network-based controller with a start-up strategy", *Advances in Intelligent Systems and*

Computing, Vol. 325, (2015), 449-457. (https://doi.org/10.1007/978-81-322-2135-7_48).

31. An, L., Franck, D. and Hameyer, K., "Sensorless field oriented control using back-EMF and flux observer for a surface mounted permanent magnet synchronous motor", *International Journal of Applied Electromagnetics and Mechanics*, Vol. 45, No. 1-4, (2014), 845-850. (https://doi.org/10.3233/JAE-141915).

32. Kazantzis, N. and Kravaris, C., "Time-discretization of nonlinear control systems via Taylor methods", *Computers & Chemical Engineering*, Vol. 23, No. 6, (1999), 763-784. (https://doi.org/10.1016/S0098-1354(99)00007-1).

33. Rodriguez, J. and Cortes, P., "Predictive control of a three-phase neutral-point clamped inverter", *Proceedings of Predictive Control of Power Converters and Electrical Drives*, *IEEE*, (2012), 65-79. (https://doi.org/10.1002/9781119941446.ch5).

34. Zhang, Z., Wang, F., Wang, J., Rodríguez J. and Kennel, R., "Nonlinear direct control for three-level NPC back-to-back converter PMSG wind turbine systems: Experimental assessment with FPGA", *IEEE Transactions on Industrial Informatics*, Vol. 13, No. 3, (2017), 1172-1183. (https://doi.org/10.1109/TII.2017.2678500).

35. Kouro, S., Cortes, P., Vargas, R., Ammann, U. and Rodriguez, J., "Model predictive control-A simple and powerful method to control power converters", *IEEE Transactions on Industrial Electronics*, Vol. 56, No. 6, (2009), 1826-1838. (https://doi.org/10.1109/TIE.2008.2008349).

36. Sazawa, M., Yamada, T., Ohishi, K. and Katsura, S., "Anti-windup algorithm with priority to proportional control output of speed PI controller for precision servo system", *Electrical Engineering in Japan (English translation of Denki Gakkai Ronbunshi)*, Vol. 170, No. 3, (2010), 57-64. (https://doi.org/10.1002/eej.20904).

37. Rodriguez, J. and Cortes, P., Predictive control of power converters and electrical drives, John Wiley & Sons, (2012), 177-190. (https://doi.org/10.1002/9781119941446.ch12).

38. Hackl, C.M., Larcher, F., Dötlinger, A. and Kennel, R.M., "Is multiple objective model-predictive control optimal?", *Proceedings of the 2013 IEEE International Symposium on Predictive Control of Electrical Drives and Power Electronics (PRECEDE)*, Munich, Germany, (2013), 1-8. (https://doi.org/10.1109/SLED-PRECEDE.2013.6684475).

39. Cortés, P., Kouro, S., La Rocca, B., Vargas, R., Rodríguez, J., León, J.I., Vazquez, S. and Franquello, L.G., "Guidelines for weighting factors design in model predictive control of power converters and drives", *Proceedings of IEEE International Conference on Industrial Technology*, (2009), 1-7. (https://doi.org/10.1109/ICIT.2009.4939742).

40. Palanisamy, R. and Krishnasamy, V., "SVPWM for 3-phase 3-level neutral point clamped inverter fed induction motor control", *Indonesian Journal of Electrical Engineering and Computer Science*, Vol. 9, No. 6, (2018), 703-710. (https://doi.org/ijeecs.v9.i3.pp703-710).

41. Bolognani, S., Petrella, R., Prearo, A. and Sgarbossa, L., "Automatic tracking of mtpa trajectory in ipm motor drives based on ac current injection", *Proceedings of IEEE Energy Conversion Congress and Exposition*, (2009), 2340-2346. (https://doi.org/10.1109/TIA.2010.2090842).